Changes in nitrate binding with lanthanides in BLPhen complexes

Th. Dhileep N. Reddy,[1] Alexander S. Ivanov,[2] Darren M. Driscoll,[2] Santa Jansone-Popova,[2] and De-en Jiang[3,*]

[1]Department of Chemistry, University of California, Riverside, CA 92521, USA

[2]Chemical Sciences Division, Oak Ridge National Laboratory, 1 Bethel Valley Road, Oak Ridge, TN 37831-6119 USA

[3]Department of Chemical and Biomolecular Engineering, Vanderbilt University, Nashville, Tennessee 37235, United States

*To whom correspondence should be addressed. E-mail: de-en.jiang@vanderbilt.edu

Abstract: Preorganized ligands such as bis-lactam-1,10-phenanthroline (BLPhen) offer unique selectivity trend in solvent extraction of rare-earth ions from their aqueous nitrate solutions, but due to their lipophilicity it is experimentally challenging to obtain crystal structures of the corresponding complexes to shed light on the structure of the first coordination shell and the role of the nitrate ions in the organic phase. Herein we report first principles molecular dynamics (FPMD) simulations of the complexation of trivalent lanthanide ions (La, Nd, and Eu) with the BLPhen ligand in the presence of nitrate ions in the dichloroethane (DCE) solvent. We find that two nitrate anions are present in the first solvation shell and the third nitrate anion is far from the first solvation shell in all three $[Ln(BLPhen)_2]^{3+}$ complexes examined. Moving along the lanthanide series from La to Nd to Eu, the binding pocket formed by the two BLPhen ligands shrinks in size; as a result, the two nitrates change from one-monodentate/one-bidentate binding mode for La and Nd to all monodentate for Eu; meanwhile, the total coordination number drops from 11 for La and Nd to 10 for Eu. More interestingly, the bidentate binding in $[La(BLPhen)_2]^{3+}$ and $[Nd(BLPhen)_2]^{3+}$ complexes is highly dynamic, frequently switching to monodentate and back. The FPMD insights into the differing modes and dynamics of nitrates in the first coordination shell will be useful for further atomistic understanding of the complex structure, formation, and stability in the organic phase.

1. Introduction

Understanding the local structure of lanthanide (Ln) complexes is essential to explain changes in their distribution ratios across the series during solvent extraction for rare-earth element (REE) separations [1,2]. The structural and thermodynamical properties depend on the nature of the solvent, ligand-metal complexation and counterions. Although many ligand-Ln complex structures have been resolved, such structures have not been available for complexes of some most recently developed ligands. A clear description of the first solvation shell, ligand-metal association, and anion approach to the complex would be desirable and molecular simulations can provide atomistic insights into such description [3–7].

The coordination of lanthanide cations to the ligands and anions is an active area of research [8–13] and REE separations are usually conducted in the presence of nitric acid. The modes of nitrate anion binding to the lanthanide cations have been extensively examined in the aqueous phase [14–18], but less so in the organic phase. When Ln(III) ions in the presence of nitric acid are extracted in the organic phase by charge-neutral ligands, some nitrate ions will accompany Ln(III) ions into the organic phase. Dichloroethane (DCE) is a commonly used organic solvent that performs well in extracting the lanthanides [19]. Therefore, it would be interesting to investigate the binding of nitrate anions to the lanthanide-ligand complex in the DCE as a typical organic solvent.

Rigid-structured ligands have recently attracted researchers in the field of REE separations [20–22]. 2,9-bis-lactam-1,10-phenanthroline (BLPhen) ligand has a rigid structure and showed one of the best selectivity towards light lanthanides [19,23], while majority of the known ligands show more selectivity towards heavy lanthanides [24]. For example, Healy et al. found that a typical BLPhen ligand in DCE can achieve separation factors of 32 for La/Nd, 398 for La/Eu, and 17326 for La/Lu in 0.9 M HNO_3 [19]. However, the atomistic description of the first solvation shell of lanthanide cations is unclear, particularly, the nitrate anion binding to the lanthanides in the organic phase. Both quantum chemical (QC) calculations with the implicit solvent model and classical molecular dynamics (CMD) simulations with explicit solvents have been used to examine REE complexes [4,23,25,26]. Implicit solvent models miss the essential interactions between complex and solvent, while CMD results highly depend on the quality of the force field and it is still challenging for the commonly used force fields to accurately describe the Ln-BLPhen complexes [26]. As such, first principles molecular dynamics (FPMD) simulations can be used to

fill the gap between QC calculations with implicit solvent models and CMD simulations with explicit solvents.

The present work investigates the effect of Ln(III) size on the nitrate coordination mode as part of the Ln-BLPhen complexes in the DCE organic solvent. Because the BLPhen ligands' preference for light lanthanides, here we focus on three typical light Ln(III) ions, namely, La(III), Nd(III), and Eu(III), given the computational cost of FPMD simulations. Our plan is to obtain a trend regarding the monodentate and bidentate binding of nitrate anions to Ln(III) and their dynamics in the DCE solvent by comparing La(III), Nd(III), and Eu(III), and then we can extend the FPMD simulations to heavier Ln(III)s and the whole series in the future. Below we first explain our computational approach.

2. Computational method

Vienna *ab initio* simulation package (VASP) was used to conduct FPMD simulations using spin-polarized density functional theory (DFT) [27,28]. Ion-electron interaction was represented by Projector augmented wave (PAW) method and standard PAW potentials were used for all the elements [29,30]. 400 eV kinetic energy cutoff was used for the plane-wave basis set. Generalized gradient approximation (GGA) of Perdew, Burke and Ernzerhof (PBE) functional was used to describe electron exchange-correlation [31]. Previous studies showed that PBE functional could well describe structure of the metal complexes in solvents [32–38]. Moreover, the PBE functional has been shown to give reliable geometries for phenanthroline derived ligands [39]; being a pure functional it is much less computationally expensive than the hybrid functionals. That is why we chose the PBE functional here, but we do note that other methods such as hybrid functionals and higher quantum chemistry methods have been used as well for phenanthroline-based ligands for metal-ion separations [35,38,40].

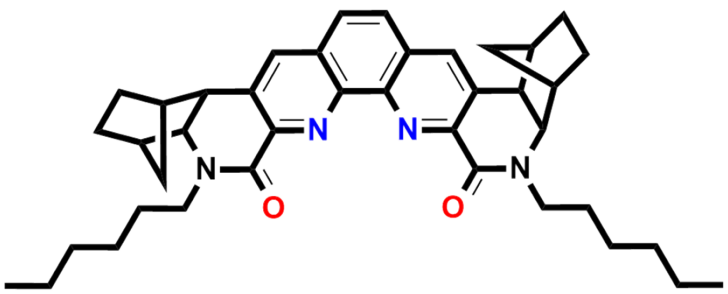

Figure 1. Molecular structure of the 2,9-bis-lactam-1,10-phenanthroline (BLPhen) derivative ligand.

The BLPhen ligand in Figure 1 can form both 1:1 and 2:1 ligand-to-metal complexes in the organic phase and recent X-ray absorption fine structure spectroscopy experiments suggest that the 2:1 complex is the dominant form [41]. So the 2:1 BLPhen:Ln(III) complexes in the DCE solvent were simulated for Ln(III) being La^{3+}, Nd^{3+}, and Eu^{3+}. 25 DCE molecules were filled in a cubic box that contained one $Ln(BLPhen)_2(NO_3)_3$ complex. The chemical structure of the BLPhen ligand employed is shown in Figure 1. Following a previous work [6], the simulation box was first equilibrated with CMD with the complex structure restrained to their DFT-optimized gas-phase geometry and then the equilibrated structure was used as the initial structure for FPMD simulations at 298 K in an NVT ensemble. During FPMD simulations, the temperature was controlled by a Nose-Hoover thermostat; 1 fs time step was used and 15 ps simulations were carried out. We started the FPMD simulations with $Nd(BLPhen)_2(NO_3)_3$ first and then repeated the simulations by replacing Nd with La and then Eu. VMD software package was used to visualize the trajectories and perform some analysis [42]. RDFs and running number integrals were calculated using TRAVIS software [43,44].

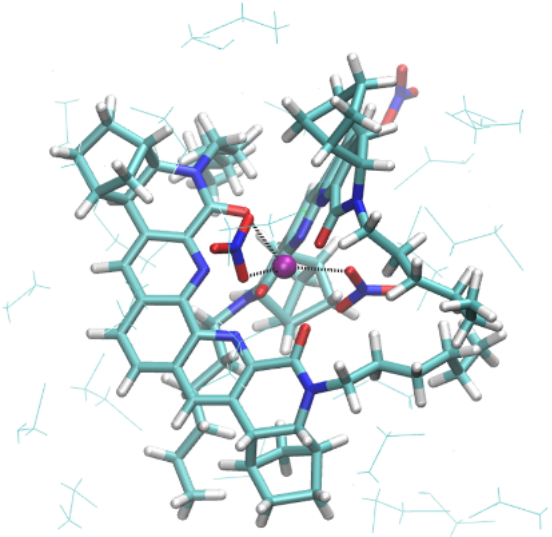

Figure 2. Snapshots BLPhen-La(III) complex in 2:1 stoichiometry in dichloroethane (DCE). DCE molecules are not shown for clarity. Color code: O, red; N, blue; Nd, pink; C, cyan; H, white.

3. Results and discussion

3.1 BLPhen-Ln interaction in the $Ln(BLPhen)_2(NO_3)_3$ complexes

Figure 2 shows a representative structure of the BLPhen:Ln 2:1 complex in the DCE solvent. Overall, the 2:1 coordination geometry is stable for all the three complexes, with two nitrates in the first coordination shell and the third one far away from the metal center. Radial distribution functions (RDFs) and number integrals between Ln(III) and the N atom in BLPhen were computed and shown in Figure 3a. The average Ln-N distances are 2.83, 2.78 and 2.70 Å for La^{3+}, Nd^{3+} and Eu^{3+} ions, respectively. The decreasing distances are consistent with the decreasing radii from La to Eu. The Ln-O(BLPhen) distances follow the same trend (Figure 3b), and are about 0.21 Å shorter than their Ln-N counterparts (Figure 4). Lanthanides are hard electron acceptors and show a higher affinity for hard donors such as O atom than the soft donors such as N [45]. Overall, the two BLPhen ligands form eight coordination bonds with the metal center.

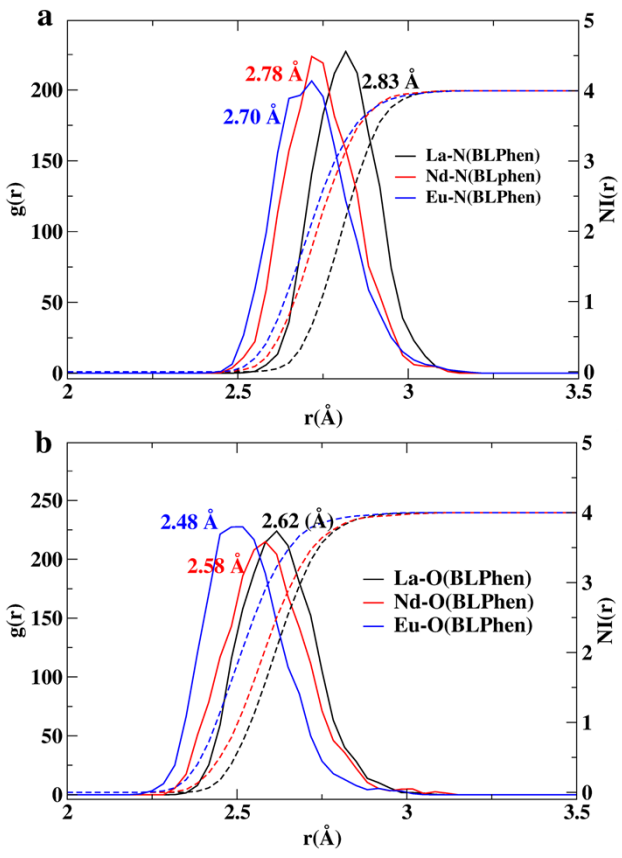

Figure 3. Atom-atom radial distribution functions (RDFs), g(r), between Ln(III) and the N/O atoms of the BLPhen ligand for the $Ln(BLPhen)_2(NO_3)_3$ complexes in the DCE solvent: (a) Ln-N(BLPhen); (b) Ln-O(BLPhen). Solid lines represent RDFs (left Y-axis) and dashed lines represent their number integration (right Y-axis), i.e., coordination number (C.N.).

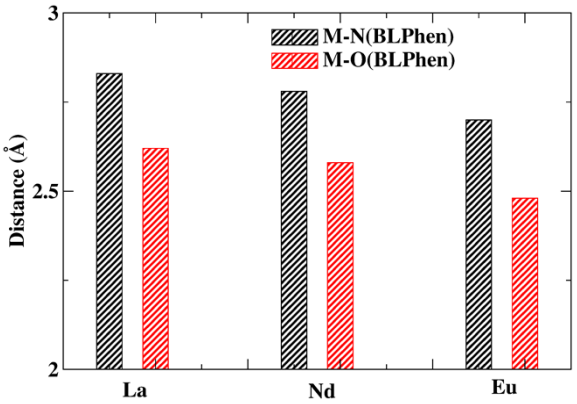

Figure 4. Average Ln-N and Ln-O distances between Ln and the BLPhen ligand for the $Ln(BLPhen)_2(NO_3)_3$ complexes in the DCE solvent, with Ln = La, Nd, and Eu.

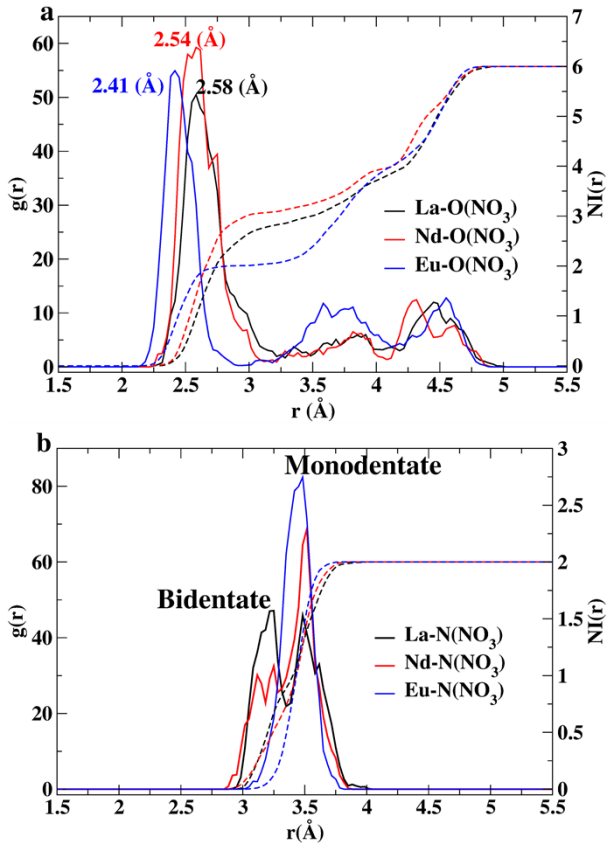

Figure 5. Atom-atom radial distribution functions, g(r), between Ln(III) and nitrate O/N atoms, for the $Ln(BLPhen)_2(NO_3)_3$ complexes in the DCE solvent: (a) Ln-$O(NO_3)$; (b) Ln-$N(NO_3)$. Solid lines correspond to g(r) (left axis); dashed lines (right axis) correspond to their number integration (NI), ie., coordination number (C.N.).

3.2. Ln(III)-nitrate interaction

Nitrate anions are also part of the complex as indicated in Figure 2. Interactions between the metal center and the two nitrates in the first-coordination shell are shown in RDFs of Ln-O (Figure 5a) and Ln-N (Figure 5b). One can see from Figure 5a that the Ln-O distances between Ln(III) and nitrate decrease from La to Eu, displaying the same trend as the distances between Ln(III) and BLPhen. More interestingly, the coordination number (C.N.) of O atoms from the two nitrates around Ln(III) at a distance cutoff of 3.0 Å clearly indicates the all-monodentate binding mode of nitrates in the Eu(III) complex (C.N.=2, meaning one atom from each nitrate) and the mixed monodentate-bidentate mode in the La(III) and Nd(III) complexes (C.N.=3, meaning one monodentate and one bidentate). This insight is further confirmed by the Ln-N RDF (Figure 5b): the all-monodentate binding mode of the two nitrates in the Eu(III) complex shows up as a single peak at 3.5 Å, while the mixed monodentate-bidentate mode of the two nitrates in the La(III) and Nd(III) complexes manifests as two different peaks at 3.2 and 3.5 Å. The 3.2-Å peak corresponds to the bidentate mode where the N center of the nitrate is closer to the metal center than that of the monodentate binding mode. One can see also the difference between the La(III) and Nd(III) complexes regarding the relative distributions of the monodentate and bidentate modes: the La(III) complex has more bidentate while the Nd(III) complex more monodentate. We quantified the distributions by the trajectory analysis: as shown in Figure 6, the bidentate mode accounts for 44% for the La(III) complex, 29% for Nd(III), and zero for Eu(III).

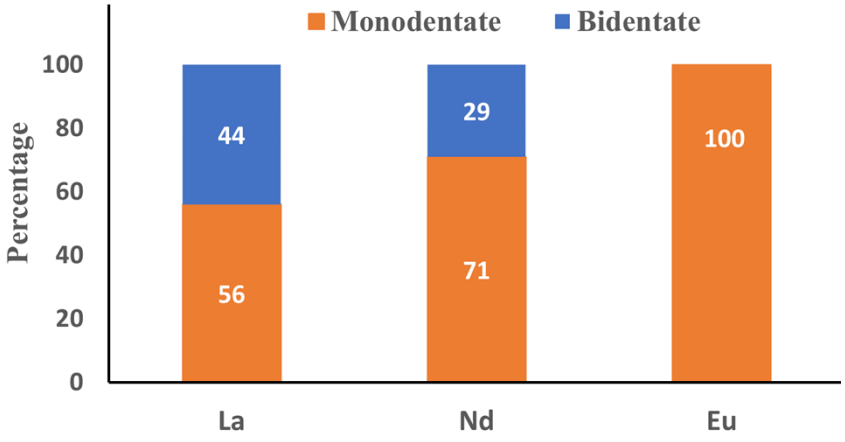

Figure 6. Percentage of monodentate and bidentate modes of the two nitrate anions in first coordination shell of the $Ln(BLPhen)_2(NO_3)_3$ complexes in the DCE solvent.

The analysis of Ln(III)-nitrate binding from Figures 5 and 6 suggests that the $[La(BLPhen)_2]^{3+}$ and $[Nd(BLPhen)_2]^{3+}$ complexes in the DCE solvent allow the bidentate nitrate anions but not $[Eu(BLPhen)_2]^{3+}$. In other words, the C.N. of the first coordination shell around the metal center is 11 for the $[La(BLPhen)_2]^{3+}$ and $[Nd(BLPhen)_2]^{3+}$ complexes but decreases to 10 for $[Eu(BLPhen)_2]^{3+}$ complex. One explanation is that the binding pocket around the metal center, formed by the two BLPhen ligands, becomes smaller from La to Eu due to the decreasing ion radii, forcing the two nitrates to become monodentate and further away from the metal center. This implies that the two nitrate anions will become more dynamic and labile from La to Eu. To examine this implication, we analyze the nitrate dynamics next.

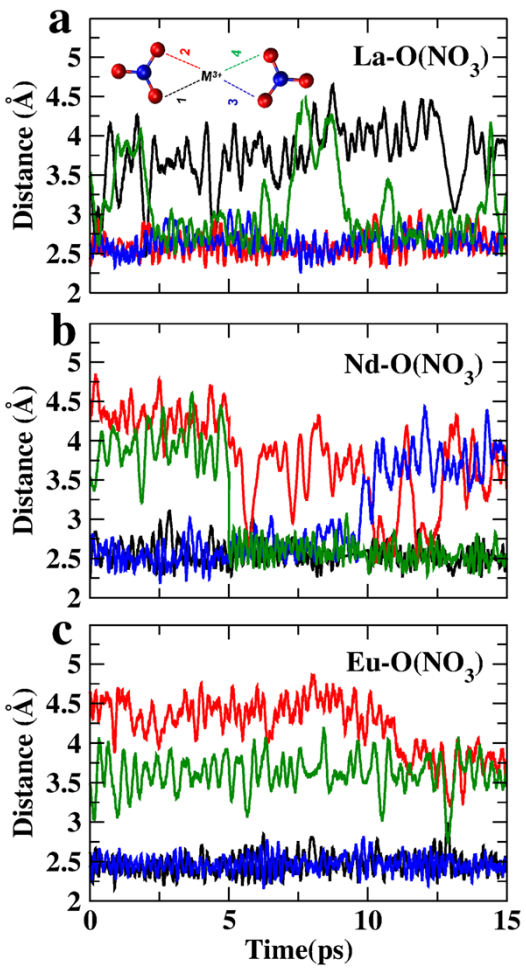

Figure 7. Time evolution of the Ln-O distances between Ln and the two nitrates in the first solvation shell of the $Ln(BLPhen)_2(NO_3)_3$ complexes in the DCE solvent.

3.3 Dynamics of the nitrate anions in the first coordination shell

We have tracked the Ln(III)-O(NO_3) distances throughout the 15 ps trajectory. As presented in Figure 7, four different oxygen atoms and their O-Ln distances are shown in four different colors. For the La(III) complex (Figure 7a), one oxygen atom stays around 4 Å most of the time (black line), meaning that this nitrate is mostly monodentate; another oxygen atom (green line) stays at 2.5 Å mostly and occasionally comes around the 4 Å. This oxygen atom represents the bidentate mode of the nitrate anion, which sometimes changes to monodentate. For the Nd(III) complex (Figure 7b), two oxygen atoms stay at 4 Å most of the time and occasionally one goes to the distance of ~2.5 Å, indicating that the two nitrate anions are monodentate at most of the time, but one of them changes to bidentate often. One also notices that the monodentate coordination bond can switch between two different O atoms of the same nitrate, for instance, from O3 (blue) to O4 (green) in the Nd(III) complex (Figure 7b). For the Eu(III) complex (Figure 7c), one can see that there are almost always two O atoms from two different nitrates at ~2.5 Å, indicating that the two nitrates are all monodentate in binding with Eu(III) predominantly; of note, transiently, one nitrate can become bidentate (for instance, at 13 ps mark in Figure 7c).

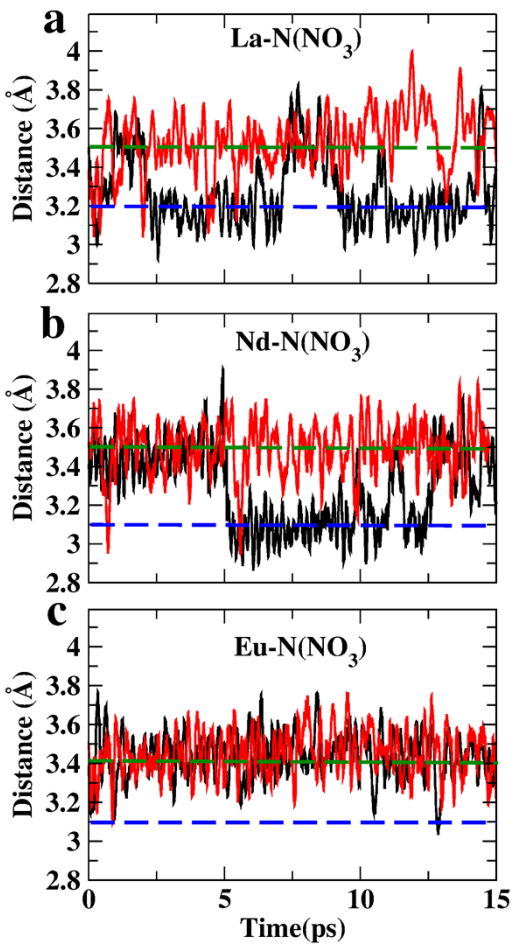

183

184 **Figure 8**. Time evolution of the Ln-N distances between Ln and the two nitrates in the first solvation
185 shell of the $Ln(BLPhen)_2(NO_3)_3$ complexes in the DCE solvent.

186

187 The differing of modes of nitrate binding from La to Eu can be more clearly seen from the
188 Ln-N distances with time: as shown in Figure 8, the shorter average Ln-N distance (3.1 – 3.2 Å,
189 blue dashed line) is for the bidentate mode, and the longer average Ln-N distance (3.4 – 3.5 Å,
190 green dashed line) for monodentate. The decreasing sampling of the bidentate mode from La to
191 Nd to Eu is apparent. Of note, occasionally the two nitrates become both bidentate in the La(III)-
192 BLPhen and Nd(III)-BLPhen complexes, while one becomes bidentate in the Eu(III)-BLPhen
193 complex, indicating the dynamic nature of the nitrate binding to the metal centers. Snapshots of
194 the most probable configurations for the three complexes are compared to Figure 9; one can see
195 that the two nitrates are at the opposite sides of the binding pocket in all three complexes.

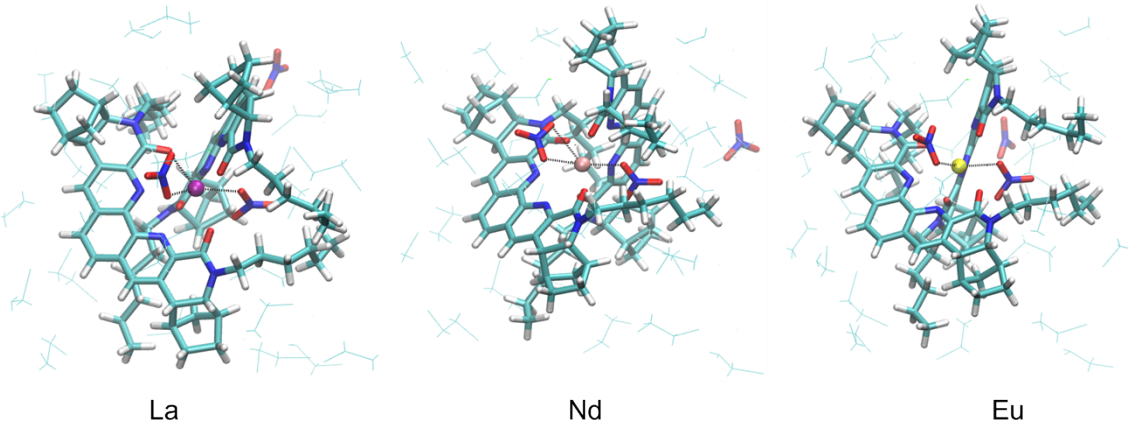

Figure 9. Snapshots of the most probable configurations of the $Ln(BLPhen)_2(NO_3)_3$ complexes in the DCE solvent. Color code: La, Violet; Nd, pink; Eu, Yellow; O, red; N, blue; C, cyan; H, white.

3.4. Implications to rare-earth separations

While the presented results are entirely based on FPMD simulations, they confirm a recent experimental spectroscopic and scattering observation of the outer-sphere nitrate binding mode in the $Nd(BLPhen)_2(NO_3)_3$ complex formed in the industrially relevant liquid–liquid extraction system [41]. There it was shown that noncoordinating nitrate anions play an important role in defining the degree of supramolecular aggregation and assembly of lanthanide complexes in the organic phase. Recent extended X-ray absorption fine structure (EXAFS) measurements have been able to confirm the 2:1 BLPhen:Nd coordination structure with four additional O atoms of nitrate anions located in the first coordination sphere [41], which agrees with the previous studies on DAPhen ligand [45]. However, X-ray absorption spectroscopy and scattering studies alone do not have the sensitivity to accurately describe the nitrate binding modes in the inner coordination sphere of the $Ln(BLPhen)_2(NO_3)_3$ complexes. Therefore, the present findings could contribute to atomistic insights into the complex formation, dynamics, and stability. In a broader context, the observed bond contraction along the Ln series accompanied by the decrease in coordination numbers could be correlated with the higher selectivity of the BLPhen ligand toward light lanthanides. Additionally, switching the nitrate binding mode from bidentate to monodentate would possibly result in the diminished strength of direct Ln-NO_3 interactions, hindering the transfer of nitrate ions from the aqueous to organic phase for charge neutralization. This in turn

might negatively affect the extraction strength of BLPhen for the heavier lanthanides, partially contributing to the observed selectivity trend.

4. Conclusions

We performed first principles molecular dynamics (FPMD) simulations of the $Ln(BLPhen)_2(NO_3)_3$ complexes in the DCE solvent for Ln being La, Nd, and Eu. Two nitrate anions are found in the first solvation shell: one nitrate is in monodentate binding mode, while the other is mainly in the bidentate model for La and Nd but changes to monodentate for Eu. The total coordination number changes from 11 for La and Nd to 10 for Eu, as the binding pocket decreases in size. The nitrate binding in $[La(BLPhen)_2]^{3+}$ and $[Nd(BLPhen)_2]^{3+}$ complexes is highly dynamic, frequently switching between bidentate and monodentate. Our work revealed the modes and dynamics of nitrate binding in the first coordination shell of $[Ln(BLPhen)_2]^{3+}$ complexes in the DCE solvent. The insights will help further understanding of the complex structure, formation, and stability in the organic phase.

Declaration of competing interest

The authors declare that they have no known competing financial interests or personal relationships that could have appeared to influence the work reported in this paper.

Acknowledgements

This work was supported by the U.S. Department of Energy, Office of Science, Office of Basic Energy Sciences, Separation Science program and Materials Chemistry program.

References

[1] T. Cheisson, E.J. Schelter, Rare earth elements: Mendeleev's bane, modern marvels, Science. 363 (2019) 489–493.

[2] F. Xie, T.A. Zhang, D. Dreisinger, F. Doyle, A critical review on solvent extraction of rare earths from aqueous solutions, Miner. Eng. 56 (2014) 10–28.

[3] A.S. Ivanov, C.J. Leggett, B.F. Parker, Z. Zhang, J. Arnold, S. Dai, C.W. Abney, V.S. Bryantsev, L. Rao, Origin of the unusually strong and selective binding of vanadium by polyamidoximes in seawater, Nat. Commun. 8 (2017) 1560.

[4] A.S. Ivanov, V.S. Bryantsev, A Computational Approach to Predicting Ligand Selectivity for the Size-Based Separation of Trivalent Lanthanides, Eur. J. Inorg. Chem. 2016 (2016) 3474–3479.

[5] X.-P. Lei, Q.-Y. Wu, C.-Z. Wang, J.-H. Lan, Z.-F. Chai, C.-M. Nie, W.-Q. Shi, Theoretical Insights into the Substitution Effect of Phenanthroline Derivatives on Am(III)/Eu(III) Separation, Inorg. Chem. 62 (2023) 2705–2714.
[6] Th.D.N. Reddy, A.S. Ivanov, D.M. Driscoll, S. Jansone-Popova, D. Jiang, Atomistic Insights into Structure and Dynamics of Neodymium(III) Complexation with a Bis-lactam Phenanthroline Ligand in the Organic Phase, ACS Omega. 7 (2022) 21317–21324.
[7] N.P. Bessen, I.A. Popov, C.R. Heathman, T.S. Grimes, P.R. Zalupski, L.M. Moreau, K.F. Smith, C.H. Booth, R.J. Abergel, E.R. Batista, P. Yang, J.C. Shafer, Complexation of Lanthanides and Heavy Actinides with Aqueous Sulfur-Donating Ligands, Inorg. Chem. 60 (2021) 6125–6134.
[8] N.C. Martinez-Gomez, H.N. Vu, E. Skovran, Lanthanide Chemistry: From Coordination in Chemical Complexes Shaping Our Technology to Coordination in Enzymes Shaping Bacterial Metabolism, Inorg. Chem. 55 (2016) 10083–10089.
[9] W.-L. Chan, C. Xie, W.-S. Lo, J.-C.G. Bünzli, W.-K. Wong, K.-L. Wong, Lanthanide–tetrapyrrole complexes: synthesis, redox chemistry, photophysical properties, and photonic applications, Chem. Soc. Rev. 50 (2021) 12189–12257.
[10] J.A. Bogart, B.E. Cole, M.A. Boreen, C.A. Lippincott, B.C. Manor, P.J. Carroll, E.J. Schelter, Accomplishing simple, solubility-based separations of rare earth elements with complexes bearing size-sensitive molecular apertures, Proc. Natl. Acad. Sci. 113 (2016) 14887–14892.
[11] A. Masuya-Suzuki, K. Hosobori, R. Sawamura, Y. Abe, R. Karashimada, N. Iki, Selective crystallization of dysprosium complex from neodymium/dysprosium mixture enabled by cooperation of coordination and crystallization, Chem. Commun. 58 (2022) 2283–2286.
[12] Z. Bai, B. Scheibe, J.M. Sperling, T.E. Albrecht-Schönzart, Syntheses and Characterization of Tetrazolate-Based Lanthanide Compounds and Selective Crystallization Separation of Neodymium and Dysprosium, Inorg. Chem. 61 (2022) 19193–19202.
[13] T.P. Gompa, S.M. Greer, N.T. Rice, N. Jiang, J. Telser, A. Ozarowski, B.W. Stein, H.S. La Pierre, High-Frequency and -Field Electron Paramagnetic Resonance Spectroscopic Analysis of Metal–Ligand Covalency in a 4f7 Valence Series (Eu2+, Gd3+, and Tb4+), Inorg. Chem. 60 (2021) 9064–9073.
[14] M. Duvail, A. Ruas, L. Venault, P. Moisy, P. Guilbaud, Molecular Dynamics Studies of Concentrated Binary Aqueous Solutions of Lanthanide Salts: Structures and Exchange Dynamics, Inorg. Chem. 49 (2010) 519–530.
[15] L. Rao, G. Tian, Complexation of Lanthanides with Nitrate at Variable Temperatures: Thermodynamics and Coordination Modes, Inorg. Chem. 48 (2009) 964–970.
[16] T. Yaita, H. Narita, Sh. Suzuki, Sh. Tachimori, H. Motohashi, H. Shiwaku, Structural study of lanthanides(III) in aqueous nitrate and chloride solutions by EXAFS, J. Radioanal. Nucl. Chem. 239 (1999) 371–375.
[17] C. Bonal, J.-P. Morel, N. Morel-Desrosiers, Interactions between lanthanide cations and nitrate anions in water. Part 1.—Effect of the ionic strength on the Gibbs energy, enthalpy and entropy of complexation of the neodymium cation, J. Chem. Soc. Faraday Trans. 92 (1996) 4957–4963.
[18] M. Dobler, P. Guilbaud, A. Dedieu, G. Wipff, Interaction of trivalent lanthanide cations with nitrate anions: a quantum chemical investigation of monodentate/bidentate binding modes, New J. Chem. 25 (2001) 1458–1465.
[19] M.R. Healy, A.S. Ivanov, Y. Karslyan, V.S. Bryantsev, B.A. Moyer, S. Jansone-Popova, Efficient Separation of Light Lanthanides(III) by Using Bis-Lactam Phenanthroline Ligands, Chem. – Eur. J. 25 (2019) 6326–6331.
[20] F.W. Lewis, L.M. Harwood, M.J. Hudson, M.G.B. Drew, J.F. Desreux, G. Vidick, N. Bouslimani, G. Modolo, A. Wilden, M. Sypula, T.-H. Vu, J.-P. Simonin, Highly Efficient Separation of Actinides from Lanthanides by a Phenanthroline-Derived Bis-triazine Ligand, J. Am. Chem. Soc. 133 (2011) 13093–13102.

[21] M. Iqbal, P.K. Mohapatra, S.A. Ansari, J. Huskens, W. Verboom, Preorganization of diglycolamides on the calix[4]arene platform and its effect on the extraction of Am(III)/Eu(III), Tetrahedron. 68 (2012) 7840–7847.
[22] H.V. Lavrov, N.A. Ustynyuk, P.I. Matveev, I.P. Gloriozov, S.S. Zhokhov, M.Y. Alyapyshev, L.I. Tkachenko, I.G. Voronaev, V.A. Babain, S.N. Kalmykov, Y.A. Ustynyuk, A novel highly selective ligand for separation of actinides and lanthanides in the nuclear fuel cycle. Experimental verification of the theoretical prediction, Dalton Trans. 46 (2017) 10926–10934.
[23] S. Jansone-Popova, A.S. Ivanov, V.S. Bryantsev, F.V. Sloop, R. Custelcean, I. Popovs, M.M. Dekarske, B.A. Moyer, Bis-lactam-1,10-phenanthroline (BLPhen), a New Type of Preorganized Mixed N,O-Donor Ligand That Separates Am(III) over Eu(III) with Exceptionally High Efficiency, Inorg. Chem. 56 (2017) 5911–5917.
[24] T. Sato, Liquid-liquid extraction of rare-earth elements from aqueous acid solutions by acid organophosphorus compounds, Hydrometallurgy. 22 (1989) 121–140.
[25] D. Manna, T.K. Ghanty, Complexation behavior of trivalent actinides and lanthanides with 1,10-phenanthroline-2,9-dicarboxylic acid based ligands: insight from density functional theory, Phys. Chem. Chem. Phys. 14 (2012) 11060–11069.
[26] M.B. Singh, Y. Fu, I. Popovs, S. Jansone-Popova, S. Dai, D. Jiang, Molecular Dynamics Simulations of Complexation of Am(III) with a Preorganized Dicationic Ligand in an Ionic Liquid, J. Phys. Chem. B. 125 (2021) 8532–8538.
[27] G. Kresse, J. Furthmüller, Efficiency of ab-initio total energy calculations for metals and semiconductors using a plane-wave basis set, Comput. Mater. Sci. 6 (1996) 15–50.
[28] G. Kresse, J. Hafner, Ab initio molecular dynamics for liquid metals, Phys. Rev. B. 47 (1993) 558–561.
[29] P.E. Blöchl, Projector augmented-wave method, Phys. Rev. B. 50 (1994) 17953–17979.
[30] G. Kresse, D. Joubert, From ultrasoft pseudopotentials to the projector augmented-wave method, Phys. Rev. B. 59 (1999) 1758–1775.
[31] J.P. Perdew, K. Burke, M. Ernzerhof, Generalized Gradient Approximation Made Simple, Phys. Rev. Lett. 77 (1996) 3865–3868.
[32] C. Priest, Z. Tian, D. Jiang, First-principles molecular dynamics simulation of the Ca2UO2(CO3)3 complex in water, Dalton Trans. 45 (2016) 9812–9819.
[33] C. Priest, B. Li, D. Jiang, Uranyl–Glutardiamidoxime Binding from First-Principles Molecular Dynamics, Classical Molecular Dynamics, and Free-Energy Simulations, Inorg. Chem. 56 (2017) 9497–9504.
[34] C. Priest, B. Li, D. Jiang, Understanding the Binding of a Bifunctional Amidoximate–Carboxylate Ligand with Uranyl in Seawater, J. Phys. Chem. B. 122 (2018) 12060–12066.
[35] S.-M. Zhang, Q.-Y. Wu, L.-Y. Yuan, C.-Z. Wang, J.-H. Lan, Z.-F. Chai, Z.-R. Liu, W.-Q. Shi, Theoretical insights into the substitution effect of phenanthroline derivative ligands on the extraction of Mo (VI), Sep. Purif. Technol. 280 (2022) 119817.
[36] M.P. Kelley, J. Su, M. Urban, M. Luckey, E.R. Batista, P. Yang, J.C. Shafer, On the Origin of Covalent Bonding in Heavy Actinides, J. Am. Chem. Soc. 139 (2017) 9901–9908.
[37] M.J. Polinski, E.B. Garner, R. Maurice, N. Planas, J.T. Stritzinger, T.G. Parker, J.N. Cross, T.D. Green, E.V. Alekseev, S.M. Van Cleve, W. Depmeier, L. Gagliardi, M. Shatruk, K.L. Knappenberger, G. Liu, S. Skanthakumar, L. Soderholm, D.A. Dixon, T.E. Albrecht-Schmitt, Unusual structure, bonding and properties in a californium borate, Nat. Chem. 6 (2014) 387–392.
[38] J.-H. Lan, W.-Q. Shi, L.-Y. Yuan, J. Li, Y.-L. Zhao, Z.-F. Chai, Recent advances in computational modeling and simulations on the An(III)/Ln(III) separation process, Coord. Chem. Rev. 256 (2012) 1406–1417.

[39] Y. Liu, C.-Z. Wang, Q.-Y. Wu, J.-H. Lan, Z.-F. Chai, Q. Liu, W.-Q. Shi, Theoretical Insights into Transplutonium Element Separation with Electronically Modulated Phenanthroline-Derived Bis-Triazine Ligands, Inorg. Chem. 60 (2021) 10267–10279.
[40] Y. Zou, J.-H. Lan, L.-Y. Yuan, C.-Z. Wang, Q.-Y. Wu, Z.-F. Chai, P. Ren, W.-Q. Shi, Theoretical Insights into Phenanthroline-Based Ligands toward the Separation of Am(III)/Eu(III), Inorg. Chem. 61 (2022) 15423–15431.
[41] D.M. Driscoll, H. Liu, B. Reinhart, I. Popovs, V. Bocharova, S. Jansone-Popova, D. Jiang, A.S. Ivanov, Noncoordinating Secondary Sphere Ion Modulates Supramolecular Clustering of Lanthanides, J. Phys. Chem. Lett. 13 (2022) 12076–12081.
[42] W. Humphrey, A. Dalke, K. Schulten, VMD: Visual molecular dynamics, J. Mol. Graph. 14 (1996) 33–38.
[43] M. Brehm, B. Kirchner, TRAVIS - A Free Analyzer and Visualizer for Monte Carlo and Molecular Dynamics Trajectories, J. Chem. Inf. Model. 51 (2011) 2007–2023.
[44] M. Brehm, M. Thomas, S. Gehrke, B. Kirchner, TRAVIS—A free analyzer for trajectories from molecular simulation, J. Chem. Phys. 152 (2020) 164105.
[45] X.-F. Yang, P. Ren, Q. Yang, J.-S. Geng, J.-Y. Zhang, L.-Y. Yuan, H.-B. Tang, Z.-F. Chai, W.-Q. Shi, Strong Periodic Tendency of Trivalent Lanthanides Coordinated with a Phenanthroline-Based Ligand: Cascade Countercurrent Extraction, Spectroscopy, and Crystallography, Inorg. Chem. 60 (2021) 9745–9756.

367 TOC

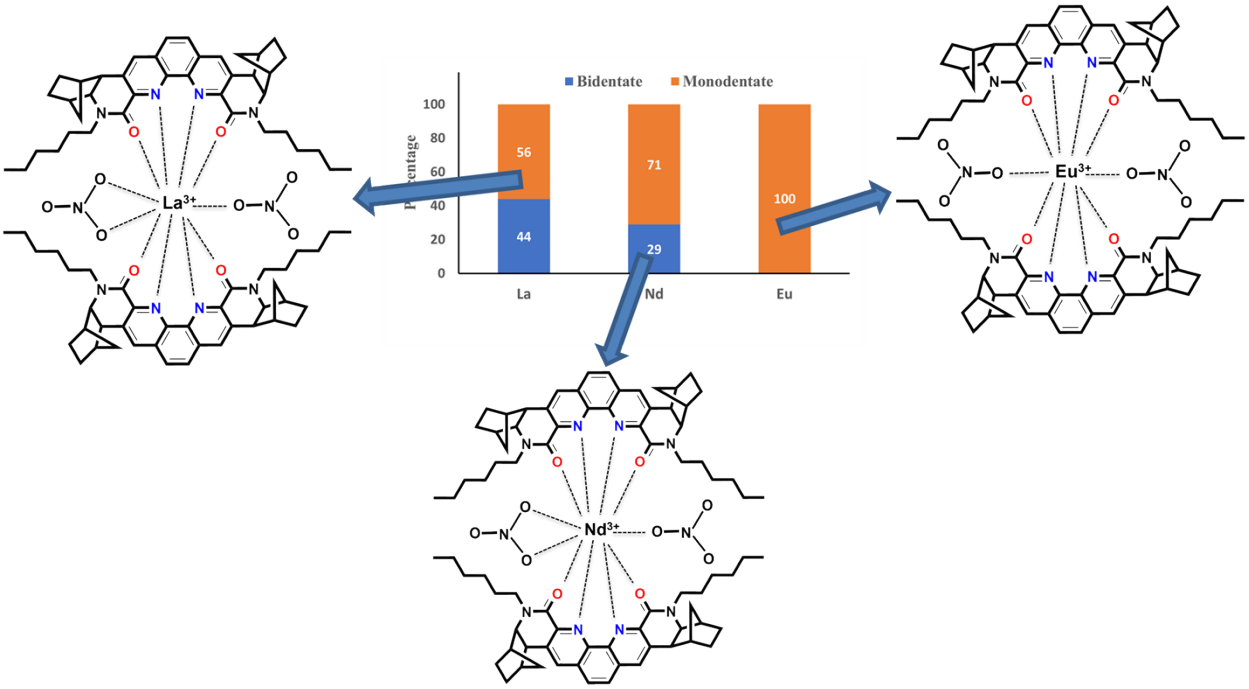
Bidentate
Monodentate
100
80
60
40
20
0
56
44
71
29
100
La
Nd
Eu
La3+
Nd3+
Eu3+

368